Agricultural and Forest Meteorology 169 (2013) 85–91

Agricultural and Forest Meteorology

journal homepage: www.elsevier.com/locate/agrformet

Can an energy balance model provide additional constraints on how to close the energy imbalance?

Georg Wohlfahrt[a,*], Peter Widmoser[b]

[a] Institute for Ecology, University of Innsbruck, Sternwartestr. 15, 6020 Innsbruck, Austria
[b] Hydrology and Water Resources Management Department, Ecology Centre, University of Kiel, Olshausenstrasse 40, 24098 Kiel, Germany

ARTICLE INFO

Article history:
Received 6 July 2012
Received in revised form 4 October 2012
Accepted 15 October 2012

Keywords:
Eddy covariance
Latent heat flux
Sensible heat flux
Available radiation
Bowen-ratio

ABSTRACT

Elucidating the causes for the energy imbalance, i.e. the phenomenon that eddy covariance latent and sensible heat fluxes fall short of available energy, is an outstanding problem in micrometeorology. This paper tests the hypothesis that the full energy balance, through incorporation of additional independent measurements which determine the driving forces of and resistances to energy transfer, provides further insights into the causes of the energy imbalance and additional constraints on energy balance closure options. Eddy covariance and auxiliary data from three different biomes were used to test five contrasting closure scenarios. The main result of our study is that except for nighttime, when fluxes were low and noisy, the full energy balance generally did not contain enough information to allow further insights into the causes of the imbalance and to constrain energy balance closure options. Up to four out of the five tested closure scenarios performed similarly and in up to 53% of all cases all of the tested closure scenarios resulted in plausible energy balance values. Our approach may though provide a sensible consistency check for eddy covariance energy flux measurements.

1. Introduction

The lack of energy balance closure, that is the sum of latent (λE) and sensible (H) heat exchange falling short of available energy (A), is a widespread problem of contemporary eddy covariance flux measurements. Available energy equals net radiation (R_N) minus the soil heat flux (G) and any other energy storage. At the majority of eddy covariance flux sites it is the rule rather than the exception to find that, on a half-hourly basis, $\lambda E + H$ underestimate A by 20–30% (Leuning et al., 2012; Wilson et al., 2002).

Given the significance of this apparently systematic bias, the energy balance closure has been studied extensively (see recent reviews by Foken, 2008; Foken et al., 2011; Leuning et al., 2012). Potential causes for the imbalance discussed in literature can be broadly categorized into four groups:

(1) *Mismatch in footprint*: Turbulent flux measurements of $\lambda E + H$ typically have footprints on the order of several hundreds of meters, while the footprint of R_N and G is typically on the order of tenth of meters to meters. While these differences in footprint, in particular at heterogeneous sites, may cause systematic differences between A and $\lambda E + H$, it is however unlikely that these differences would lead to a systematic overestimation of A and underestimation of $\lambda E + H$ at the majority of sites (Foken, 2008).

(2) *Measurement/calculation errors*: While there is variability between different models of net radiometers of different manufacturers, a recent review by Leuning et al. (2012) arrives at the conclusion that these differences are not able to account for the observed systematic differences between A and $\lambda E + H$. In contrast, Leuning et al. (2012), suggest that neglecting parts of the heat storage accounts for an appreciable fraction of the observed energy imbalance. Comparing half-hourly and daily averaged, when changes in heat storage should cancel, energy balance closures, the energy imbalance improved from an underestimation of 25% to 10%. Similarly, better energy balance closure has been reported for improved methods of soil heat flux calculation (Heusinkveld et al., 2004), heat storage in biomass (Lindroth et al., 2010) and taking into account the energy stored in metabolic processes (Jacobs et al., 2008). Errors in the vertical wind component due to sonic anemometer design (Kochendorfer et al., 2012; Nakai and Shimoyama, 2012) or contamination by horizontal velocity components (Leuning et al., 2012) have been shown to cause an underestimation of sensible and latent heat flux measurements. A systematic underestimation of latent and sensible heat fluxes also occurs if not corrected for effects of low- and high-pass filtering or density fluctuations (Leuning et al., 2012; Massman, 2000; Mauder and Foken, 2006).

* Corresponding author. Tel.: +43 0 512 5075977; fax: +43 0 512 5072975.
E-mail address: georg.wohlfahrt@uibk.ac.at (G. Wohlfahrt).

0168-1923
http://dx.doi.org/10.1016/j.agrformet.2012.10.006

(3) *Advective flux divergence*: Horizontal and vertical advective flux divergence, neglected at most eddy covariance flux sites, may contribute to the energy imbalance, although Leuning et al. (2012) have shown that unrealistically large horizontal and/or vertical temperature and moisture gradients need to be invoked in order to explain typical midday energy imbalances of >100 J m^{-2} s^{-1}. It also should be noted that any advective flux divergence may cause a net import and/or export of energy (Finnigan, 1999), and it is thus again difficult to explain the observed systematic underestimation of $\lambda E + H$ with respect to A (Leuning et al., 2012).

(4) *Inadequate sampling of low frequency/large scale turbulent motions*: Turbulent transport at larger spatial/longer temporal scales not captured by typical half-hourly averaging times at a single tower have been shown to cause a systematic underestimation of sensible and latent heat fluxes on the order of 30% (Finnigan et al., 2003; Leuning et al., 2012; Mauder and Foken, 2006). These findings are corroborated by large eddy simulations (Kanda et al., 2004), spatially distributed eddy covariance measurements (Mauder et al., 2008) and area-averaging flux measurement methods such as scintillometry (Beyrich et al., 2006). Over short vegetation, however, underestimation of low frequency flux contributions appears to represent a minor issue (Foken et al., 2011).

In summary, past research has identified several potential causes for $A \neq \lambda E + H$, some of which also explain the systematic underestimation of $\lambda E + H$ with respect to A. Given the vast variability between sites in the factors that have the potential to contribute to the energy imbalance, such as measurement equipment and deployment, data post-processing, site topography and heterogeneity, ecosystem structure and so forth, it is however likely that no single cause is able to universally explain the imbalance.

The energy imbalance, on one hand, represents a theoretical problem as it violates the law of energy conservation. There are however also practical aspects to this problem which greatly limit the usefulness of eddy covariance energy flux measurements: The residual energy, $\varepsilon = A - (\lambda E + H)$, causes problems when using the measured energy balance components to calibrate/validate models that are based on the law of energy conservation, i.e. implicitly assume the energy balance to be closed (Williams et al., 2009). For example, Wohlfahrt et al. (2009) noted that widely varying estimates for the surface conductance to water vapor were obtained by inverting the Penman–Monteith combination equation depending on how ε was dealt with. A similar problem arises when measured evapotranspiration rates (i.e. the latent heat flux divided by the latent heat of vaporization) are used as input to a water budget model (e.g. Williams et al., 2012). In the simplest case such a water budget model would assume that precipitation (P) is consumed by evapotranspiration (ET) and runoff (R), i.e. $P = ET + R$, and it is clear that for a given P any errors in ET will propagate into R estimates. It should be mentioned that if ε is to be attributed to errors in λE and/or H, other scalar fluxes measured with the eddy covariance technique, e.g. carbon dioxide fluxes (Baldocchi, 2008), are likely to be underestimated as well.

For applications that require a closed energy balance, it may thus be desirable to force energy balance closure, i.e. attribute the residual energy to A, λE, H or combinations thereof. However, since a general solution to the 'energy balance problem' remains elusive, there is no generally accepted approach for doing so. Twine et al. (2000) suggested adjusting both λE and H according to the average energy imbalance. This approach, which was employed recently in a global analysis of evapotranspiration (Jung et al., 2010), conserves the Bowen-ratio (β) and closes the energy balance on average, however results in a (small) residual ε on the half-hourly time step. Wohlfahrt et al. (2009, 2010) additionally explored forcing energy balance closure by adjusting H, λE and A separately and by adjusting H and λE every half-hour so that β remains unchanged. However, even when independently measured evapotranspiration estimates were available, none of these closure options did clearly outperform the others (Wohlfahrt et al., 2010). Note that with models that assume a closed energy balance, using the energy balance components as measured may equate to unintentionally forcing energy balance closure. For example, Wohlfahrt et al. (2009) demonstrated that using the Penman–Monteith combination equation expressed in terms of A and λE amounts to implicitly allocating ε to H, while if it is expressed in terms of β the residual is distributed to H and λE in proportion to β.

So far, at least to the best of our knowledge, no attempt has been made to investigate whether additional constraints allow further insights into how to best force energy balance closure and thus in turn shed light on the causes underlying the energy imbalance. A logical starting point for doing so is to use the full energy balance, as detailed in the next section, to investigate the biological/physical plausibility of various closure options. With "full energy balance" we mean that the drivers of and resistances to the latent and sensible heat exchange are explicitly represented.

The objective of the present paper is to explore whether by using the full energy balance equation as an additional constraint, further insights into the plausibility of closure options can be gained. To this end we make use of the theoretical framework developed by Widmoser (2009, 2010), which makes less assumptions compared to the frequently used Penman–Monteith combination equation (Monteith, 1965) and conveniently allows to separate biologically/physically plausible from implausible solutions. Field data from three different study sites, a temperate mountain grassland, a Mediterranean cork oak plantation and a desert shrub ecosystem are used to test and illustrate our approach.

2. Methods

2.1. Theoretical background

The method used in this paper to separate plausible energy closures from biologically/physically unrealistic ones is based on theoretical developments by Widmoser (2009, 2010), which is briefly summarized in the following.

One way of extending the energy balance, i.e.

$$A = R_N - G = \lambda E + H, \tag{1}$$

where R_N, G, λE and H represent the net radiation, soil heat flux, latent and sensible heat fluxes (all units: J m^{-2} s^{-1}) respectively, is to write:

$$A = [e_s(T_s) - e_a]\frac{c_v}{\gamma(T_s) r_v} + [T_s - T_a]\frac{c_v}{r_H} \tag{2}$$

Here $e_s(T_s)$ and e_a refer to the saturation vapor pressure at the surface temperature and the actual air vapor pressure (Pa), T_s and T_a to the surface and air temperature (°C), c_v to the volumetric heat capacity of moist air at constant pressure (J m^{-3} K^{-1}), $\gamma(T_s)$ to the psychrometric parameter (Pa K^{-1}) as a function of T_s, and r_v and r_H to the surface resistance to water vapor and heat transfer (m s^{-1}).

In Eqs. (1) and (2) the values A, λE, H, T_a, e_a and r_H are assumed to have been directly measured or inferred from measurements through additional models (r_H). Separating the terms with T_s and setting r_H equal to the aerodynamic resistance r_a and r_v equal to the sum of $r_a + r_c$ (r_c = canopy (stomatal) resistance to vapor transport) leads to

$$\frac{e_s(T_s)}{r_1 \gamma(T_s)} + T_s = T_a + A\frac{r_a}{c_v} + \frac{e_a}{r_1 \gamma(T_a)}, \tag{3}$$

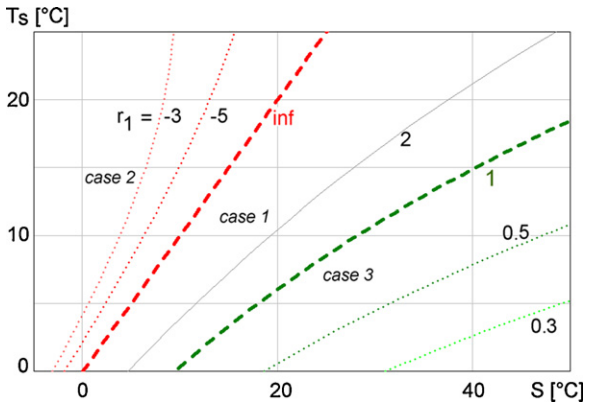

Fig. 1. T_s–S–r_1 diagram for various r_1-values. Thick, dashed lines to the left ($r_1 = \infty$; upper bound) and to the right ($r_1 = 1$; lower bound), border the physically plausible region of the diagram.

where

$$r_1 = \frac{r_a + r_c}{r_a} = \frac{e_s(T_s) - e_a}{\gamma(T_s)} \left[A \frac{r_a}{c_v} - T_s + T_a \right]^{-1}. \quad (4)$$

The right-hand side of Eq. (3) may be lumped into the parameter S (°C):

$$S = T_a + A \frac{r_a}{c_v} + \frac{e_a}{r_1 \gamma(T_a)}. \quad (5)$$

Since S combines the physiological term r_c (as part of r_1) with relevant meteorological data, it may be considered a physio-meteorological parameter.

T_s is obtained from

$$T_s = T_a + H \frac{r_a}{c_v}. \quad (6)$$

The functional relations between S, T_s and r_1 may be presented in a T_s–S–r_1 diagram (Fig. 1) by using

$$S(T_s) = \frac{e_s(T_s)}{r_1 \gamma(T_s)} + T_s. \quad (7)$$

which follows from Eqs. (3) and (5).

The T_s–S–r_1 diagram (Fig. 1) is obtained by inserting T_s-values within a meteorological plausible range into Eq. (7) and keeping selected values for r_1 constant. For $r_1 \to \infty$ (i.e. $r_c \to \infty$ or $r_a \to 0$), $S(T_s)$ becomes equal to T_s, represented by a straight line with a slope of unity (the left, upper bound). For $r_1 = 1$ (the right, lower bound) one may also use an approximation, where $T_s(S)$ is a function of S as given by Eq. (10) in Widmoser (2010).

The region framed between the upper and lower boundaries defined above will be called the *plausible region* of the diagram (case 1). It can be shown that negative r_1-values are left to the upper (case 2) and values $0 \le r_1 < 1$ are right to the lower boundary (case 3). Cases 1–3 are defined for closed systems by the following:

Case 1, i.e. $r_1 \ge 1$ and thus plausible values, only occur if

$$\frac{|VPD(T_s)|}{\gamma(T_s)} \ge |\lambda E| \frac{r_a}{c_v} \cap sgn(VPD(T_s)) = sgn(\lambda E), \quad (8)$$

where $VPD(T_s) = e_s(T_s) - e_a$.

Note that Eq. (8) suggests evaporation for positive and condensation for negative signs of λE and $VPD(T_s)$.

Case 2, i.e. ($r_1 < 0$), only occurs if

$$sgn(VPD(T_s)) \ne sgn(\lambda E), \quad (9)$$

in other words if the sign of the latent heat flux and its environmental driving force do not match.

Case 3, i.e. $0 \le r_1 < 1$, only occurs if

$$\frac{|VPD(T_s)|}{\gamma(T_s)} < |\lambda E| \frac{r_a}{c_v} \cap sgn(VPD(T_s)) = sgn(\lambda E). \quad (10)$$

Typically, this is the case with large r_a and/or λE values.

In addition it was found that among the plausible values, i.e. case 1 above, unrealistically large surface to air temperature gradients occurred when H and/or r_a were too large (Eq. (6)). In a first step, case 1 values were thus further filtered for $|T_s - T_a| \le 20$ °C.

Table 1
Scenarios for forcing energy balance closure, i.e. weight combinations (Eqs. (11a)–(11c)) used and the respective closure names.

$w_{\lambda E}$	w_H	w_A	Closure name
1	0	0	λE
0	1	0	H
0	0	1	A
1/3	1/3	1/3	Balanced (1/3)
Eq. (12a)	Eq. (12b)	0	β

2.2. Scenarios for forcing energy balance closure

Closing the energy imbalance was done by distributing ε to the three energy balance components, A, λE and H, in weighted portions (w), so that the adjusted values (marked with a *) become

$$\lambda E^* = \lambda E + w_{\lambda E} \varepsilon, \quad (11a)$$

$$H^* = H + w_H \varepsilon, \quad (11b)$$

$$A^* = A - w_A \varepsilon, \quad (11c)$$

where the sum of the weights equals unity. As there exists an infinite number of possible weight combinations, we focus on five scenarios as summarized in Table 1. Three closure scenarios, where ε is attributed entirely to λE, H or A, are used to explore extreme closure options. These are complemented by two moderate scenarios – one where ε is distributed equally to the three energy balance components (balanced closure) and another one where ε is assigned to λE and H (i.e. $w_A = 0$) so that β is preserved (Wohlfahrt et al., 2009). In the latter case the weights are calculated as:

$$w_{\lambda E} = 1 - w_H, \quad (12a)$$

$$w_H = \frac{\beta(\lambda E + \varepsilon) - H}{\varepsilon(1 + \beta)}. \quad (12b)$$

Note that the β-closure becomes unstable when β approaches -1. The average imbalance closure proposed by Twine et al. (2000) is not explored as it results in a residual ε at the half-hourly time scale which then needs to be closed by some other approach.

The following provides a step-by-step description of the procedure: (1) compute ε as $A - (\lambda E + H)$ and distribute it to λE, H and/or A according to selected closure scenario (Table 1); (2) use Eq. (6) to calculate T_s; use T_s to calculate r_1 (Eq. (4)) and both to calculate S (Eq. (5)); (3) plot pairs of T_s and S in T_s–S–r_1-diagram (Fig. 1) and assign data to cases 1–3 based on r_1. Fig. 2 gives examples, for the times of sunrise, noon and sunset at the study site Neustift that are meant to illustrate how the investigated closure scenarios affect the location in the T_s–S–r_1-diagram. In this example all data are located in the plausible range (case 1), except for the λE-closure during sunrise (case 2) and sunset (case 3) and the β-closure during sunset (case 2). The effect the different closure scenarios have on the location in the T_s–S–r_1-space, i.e. whether closure scenarios fall into the plausible range or not, will be used in the following to

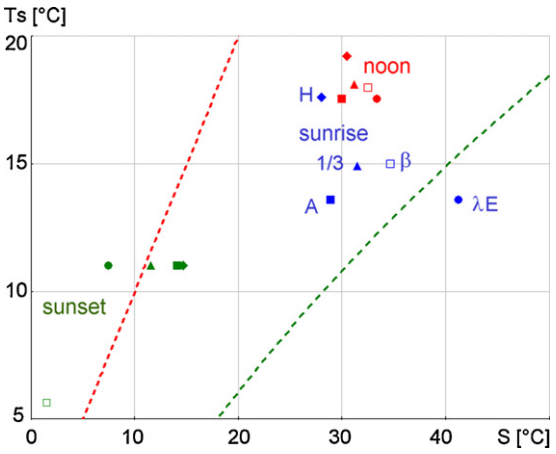

Fig. 2. Illustrative examples (using half-hourly data from sunrise, noon and sunset from the study site Neustift) for the effects of the tested closure scenarios (λE, H, A, 1/3 and β; Table 1) in the T_s–S–r_1 diagram.

diagnose possible biological/physical limits to the magnitude of A, λE and H.

2.3. Experimental data

Three data sets from a temperate mountain grassland (Neustift) in Austria, a Mediterranean cork oak (*Quercus suber*) plantation (Rio Frio) in Portugal and a desert shrub ecosystem (Mojave) in the US are used to test and illustrate our approach. As these data have been published previously we refer to the respective publications for further details on site characteristics and methods (Hammerle et al., 2008; Nadezhdina et al., 2008; Wohlfahrt et al., 2008, 2009). Briefly, λE and H were measured by means of the eddy covariance method (Aubinet et al., 2000; Baldocchi et al., 1988), R_N, G, T_a and e_a by standard micrometeorological methods. The aerodynamic resistance (r_a), c_v and γ were calculated according to Ham (2005). The measured soil heat flux was corrected for the energy storage above the heat flux plates based on the calorimetric method (Sauer and Horton, 2005). Data from Neustift cover the period of May 2006, Rio Frio 10 days in July 2003, and Mojave March 2006.

3. Results

Energy balance closure, based on half-hourly data, at the three study sites ranged from an underestimation of 18% at Neustift ($\lambda E + H = 0.82A - 3.7$; $r^2 = 0.90$) and Mojave ($\lambda E + H = 0.82A + 13.7$; $r^2 = 0.64$) to 8% at Rio Frio ($\lambda E + H = 0.92A + 9.2$; $r^2 = 0.95$). During an average diurnal course ε varied from an overestimation of −70 to an underestimation of +130 J m^{-2} s^{-1} at Neustift, −90 to +73 J m^{-2} s^{-1} at Mojave and −24 to +78 J m^{-2} s^{-1} at Rio Frio (Fig. 3). Note the hysteresis in ε during the morning (overestimation) and afternoon (underestimation) hours at Mojave (Fig. 3).

Forcing energy balance closure by assigning ε solely to λE resulted in the least fraction of plausible values at all sites (42–51% implausible values; Fig. 4). The largest fractions of plausible values (>70%) were obtained with the H- and A-closures at all sites and the balanced (1/3) and β-closures at Neustift and Mojave (Fig. 4). Implausible values were mostly (7–41%) due to $r_1 < 0$ (case 2; Fig. 4). As shown in Fig. 5, $r_1 < 0$ was most frequently observed during nighttime conditions, when λE was generally around zero and any closure operation may easily cause $\mathrm{sgn}(VPD(T_s)) \neq \mathrm{sgn}(\lambda E)$. The exception to this was Mojave, where the λE-closure caused $r_1 < 0$ from early morning till noon (Fig. 5). Recall that at this site ε was negative, i.e. overestimation of $\lambda E + H$ with respect to A, during the morning (Fig. 3) and therefore the λE-closure caused a small positive λE to become negative, violating $VPD(T_s) > 0$ typical for this time of the day. With the exception of the λE-closure at Neustift and Mojave, case 3, i.e. $0 \leq r_1 < 1$, contributed a relatively small (0–9%) fraction to the implausible values (Fig. 4), generally associated with large r_a values (Eq. (10)). At Neustift and Mojave, the condition for $0 \leq r_1 < 1$, i.e. Eq. (10), was fulfilled by assigning ε solely to λE (λE-closure) in 27 and 17% of all cases (Fig. 4). Unrealistically large surface to air temperature gradients ($|T_s - T_a| > 20$ °C) were caused by any closure scenario in 2–9% of all cases at Neustift and Mojave and never at Rio Frio (Figs. 4 and 5).

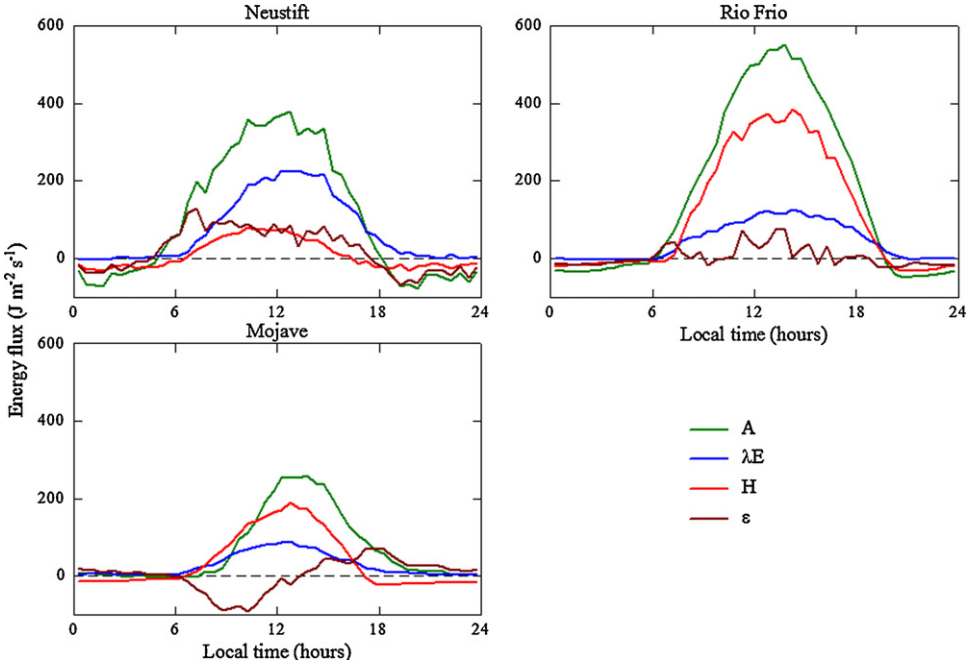

Fig. 3. Bin-averaged diurnal courses of the available energy (A), the latent (λE) and sensible (H) heat fluxes and the residual energy (ε) at the three study sites. A positive ε indicates an underestimation of $\lambda E + H$ with respect to A and vice versa.

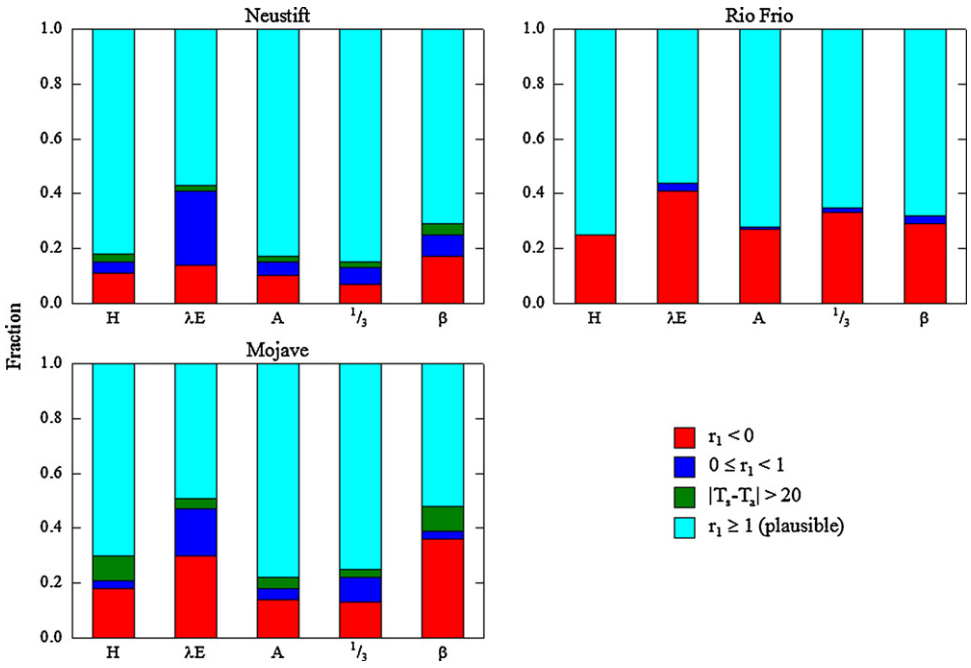

Fig. 4. Fraction of biologically/physically plausible and implausible (according to Widmoser, 2009, 2010) energy balance solutions for different closure scenarios.

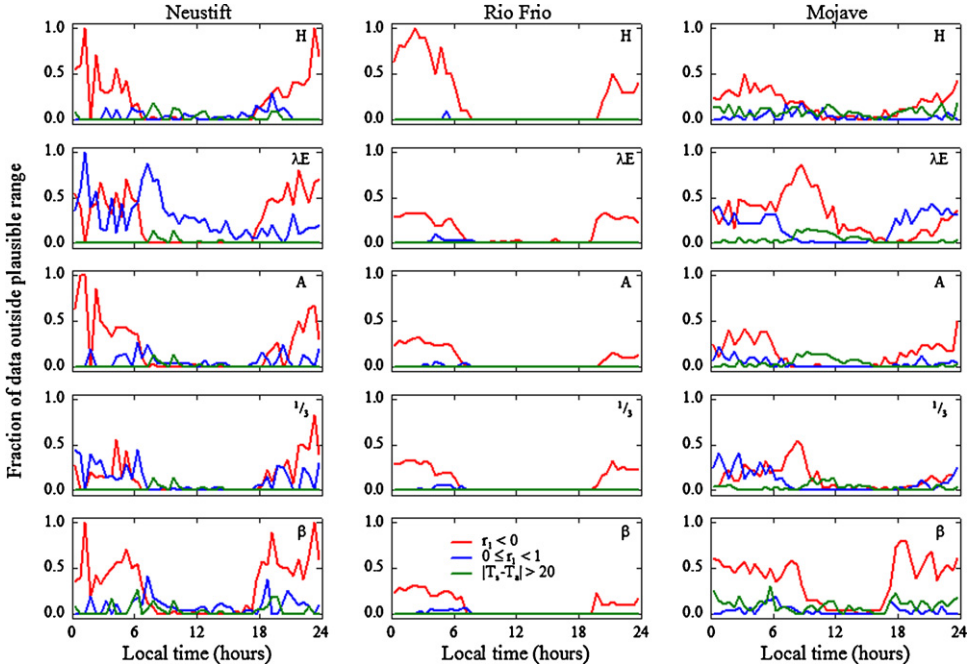

Fig. 5. Mean diurnal variation of the fraction of biologically/physically implausible (according to Widmoser, 2009, 2010) energy balance solutions for different closure scenarios. Biologically/physically plausible solutions can be inferred from 1 minus the fraction of implausible ones.

In 36–53% of all measurements, in particular during daytime, all of the tested closure scenario produced plausible values, while in 6–23% of all measurements, generally during nighttime, none of the scenarios resulted in plausible values.

4. Discussion

The objective of the present paper was to test whether the full energy balance equation provides additional constraints on the energy imbalance that allow further insights into the plausibility of various energy balance closure scenarios and thus possibly on the causes underlying the imbalance. To this end we used the energy balance in the form proposed by Widmoser (2009, 2010) as it based on fewer assumptions as compared to the well-known Penman–Monteith combination equation (Monteith, 1965) and provides a convenient framework for identifying and diagnosing implausible closure scenarios.

The main finding of our study is that despite adding additional independent information, the full energy balance, i.e. Eq. (2), offers limited insights into how to best force closure of the energy imbalance. Overall, up to four, i.e. the *H*-, *A*-, balanced and *β*-closure,

out of the five closure scenarios tested performed similarly in closing the energy balance (Fig. 4) and in up to 53% of all cases all of the tested closure scenarios resulted in plausible energy balance values. Values outside the biologically/physically plausible range (Fig. 1) mostly occurred during nighttime, when energy fluxes are typically small and characterized by large relative random uncertainties (Richardson et al., 2006) that may readily cause implausible results. Thus during daytime, when the energy imbalance is most prominent and ε often exceeds 100 J m^{-2} s^{-1} (Fig. 3), none of the closure scenarios clearly outperformed the others. A similar conclusion was reached by Wohlfahrt et al. (2010) using independent λE measurements for constraining energy balance closure options at Neustift.

The only closure scenario that resulted in a clearly smaller fraction of plausible values was the λE-closure, which assigns ε entirely to λE (Table 1), and at Neustift and Mojave caused an appreciable fraction of rejected daytime values (Fig. 5). At Mojave the large number of implausible values in the morning (Fig. 5) was due to $A < \lambda E + H$, which caused the λE-closure to turn λE from small positive to negative numbers during times with a positive $VPD(T_s)$, which in the framework of Widmoser (2009, 2010) and leads to $r_1 < 0$ (Eq. (9)), i.e. case 2. In contrast, at Neustift the λE-closure increased λE to a degree that the condition of Eq. (10), i.e. $VPD(T_s)\,\gamma(T_s)^{-1} < r_a\,\lambda E\,c_v^{-1}$ (case 3), became true. The larger fraction of implausible values with the λE-closure implies that it is unlikely that ε is entirely attributable to λE. While this does not imply that λE is being measured correctly, as shown by independent measurements of evapotranspiration (e.g. Chávez et al., 2009; Wohlfahrt et al., 2010), this finding indicates physical bounds for λE during daytime conditions, which was not the case for the other closure scenarios that adjust λE (balanced and β-closure; Table 1).

The two examples above suggest that the causes for the energy imbalance are likely to be, at least to a certain degree, site-specific and depend on instrument type/deployment, data post-processing, site characteristics and so forth. For example, from Fig. 3 it appears that the hysteresis in ε at Mojave may be linked to a phase shift in A, which Leuning et al. (2012) argued to be a major contributor to ε.

The fact that in up to 23% of cases all of the investigated closure scenarios produced implausible values, indicates for the affected data a general discrepancy between the measured energy balance components (A, λE and H), the additional independent measurements embodied in Eq. (2) and the energy balance itself. While this mismatch happened most frequently during nighttime conditions and may be explained by the above-mentioned large relative measurement uncertainties, generally testing data for such discrepancies may provide a valuable additional quality check, for example during the standardized processing of energy flux data in the FLUXNET network of eddy covariance sites (Papale et al., 2006).

Taken together, our approach of using the full energy balance fails to provide the hypothesized additional constraints on how to best close the energy imbalance during daytime, when it is quantitatively most severe, and is thus not able to support/reject any of the potential causes discussed in literature. The energy imbalance thus remains an outstanding problem in micrometeorology and continuing efforts by the scientific community are required in order to make progress on this subject.

Acknowledgements

Data collection at Neustift was financially supported by the Austrian National Science Fund (P23267-B16, P17560-B03), the Tyrolean Science Fund (UNI-404-33) and the University of Innsbruck. A. Hammerle, A. Haslwanter and L. Hörtnagl (University of Innsbruck) are acknowledged for assistance with data collection and processing. We thank A. Pitacco (University of Padova), R. Vogt (University of Basel) and I. Ferreira (University of Lisbon) for supplying the Rio Frio data which were collected under the EU project WATERUSE (EVK1-2000-00079EU). We gratefully acknowledge Mojave Desert shrub data provided by the Desert Research Institute (J. Arnone, L. Fenstermaker and R. Jasoni) that were supported by a DOE Terrestrial Carbon Processes program grant (DE-FG02-03ER63651) and funding from DRI, UNLV and UNR.

References

Aubinet, M., Grelle, A., Ibrom, A., Rannik, Ü., Moncrieff, J., Foken, T., Kowalski, A.S., Martin, P.H., Berbigier, P., Bernhofer, C., Clement, R., Elbers, J., Granier, A., Grünwald, T., Morgenstern, K., Pilegaard, K., Rebmann, C., Snijders, W., Valentini, R., Vesala, T., 2000. Estimates of the annual net carbon and water exchange of forests: the EUROFLUX methodology. Adv. Ecol. Res. 30, 113–175.

Baldocchi, D., 2008. Turner Review No. 15. 'Breathing' of the terrestrial biosphere: lessons learned from a global network of carbon dioxide flux measurement systems. Aust. J. Bot. 56 (1), 1–26.

Baldocchi, D.D., Hincks, B.B., Meyers, T.P., 1988. Measuring biosphere–atmosphere exchanges of biologically related gases with micrometeorological methods. Ecology 69 (5), 1331–1340.

Beyrich, F., Leps, J.-P., Mauder, M., Bange, J., Foken, T., Huneke, S., Lohse, H., Lüdi, A., Meijninger, W., Mironov, D., Weisensee, U., Zittel, P., 2006. Area-averaged surface fluxes over the Litfass region based on Eddy-covariance measurements. Bound. Layer Meteorol. 121 (1), 33–65.

Chávez, J., Howell, T., Copeland, K., 2009. Evaluating eddy covariance cotton ET measurements in an advective environment with large weighing lysimeters. Irrigation Sci. 28 (1), 35–50.

Finnigan, J., 1999. A comment on the paper by Lee (1998): on micrometeorological observations of surface-air exchange over tall vegetation. Agric. Forest Meteorol. 97 (1), 55–64.

Finnigan, J.J., Clement, R., Malhi, Y., Leuning, R., Cleugh, H.A., 2003. A re-evaluation of long-term flux measurement techniques Part I: averaging and coordinate rotation. Bound. Layer Meteorol. 107 (1), 1–48.

Foken, T., 2008. The energy balance closure problem: an overview. Ecol. Appl. 18 (6), 1351–1367.

Foken, T., Aubinet, M., Finnigan, J.J., Leclerc, M.Y., Mauder, M., Paw U, K.T., 2011. Results of a panel discussion about the energy balance closure correction for trace gases. Bull. Am. Meteorol. Soc. 92 (4), ES13–ES18.

Ham, J.M., 2005. Useful equations and tables in micrometeorology. In: Hatfield, J.L., Baker, J.M., Viney, M.K. (Eds.), Micrometeorology in Agricultural Systems. American Society of Agronomy Inc./Crop Science Society of America Inc./Soil Science Society of America Inc., Madison, WI, USA, pp. 533–560.

Hammerle, A., Haslwanter, A., Tappeiner, U., Cernusca, A., Wohlfahrt, G., 2008. Leaf area controls on energy partitioning of a temperate mountain grassland. Biogeosciences 5 (2), 421–431.

Heusinkveld, B.G., Jacobs, A.F.G., Holtslag, A.A.M., Berkowicz, S.M., 2004. Surface energy balance closure in an arid region: role of soil heat flux. Agric. Forest Meteorol. 122 (1–2), 21–37.

Jacobs, A., Heusinkveld, B., Holtslag, A., 2008. Towards closing the surface energy budget of a mid-latitude grassland. Bound. Layer Meteorol. 126 (1), 125–136.

Jung, M., Reichstein, M., Ciais, P., Seneviratne, S.I., Sheffield, J., Goulden, M.L., Bonan, G., Cescatti, A., Chen, J., de Jeu, R., Dolman, A.J., Eugster, W., Gerten, D., Gianelle, D., Gobron, N., Heinke, J., Kimball, J., Law, B.E., Montagnani, L., Mu, Q., Mueller, B., Oleson, K., Papale, D., Richardson, A.D., Roupsard, O., Running, S., Tomelleri, E., Viovy, N., Weber, U., Williams, C., Wood, E., Zaehle, S., Zhang, K., 2010. Recent decline in the global land evapotranspiration trend due to limited moisture supply. Nature 467 (7318), 951–954.

Kanda, M., Inagaki, A., Letzel, M.O., Raasch, S., Watanabe, T., 2004. LES study of the energy imbalance problem with eddy covariance fluxes. Bound. Layer Meteorol. 110 (3), 381–404.

Kochendorfer, J., Meyers, T., Frank, J., Massman, W., Heuer, M., 2012. How well can we measure the vertical wind speed? Implications for fluxes of energy and mass. Bound. Layer Meteorol. 145, 383–398.

Leuning, R., van Gorsel, E., Massman, W.J., Isaac, P.R., 2012. Reflections on the surface energy imbalance problem. Agric. Forest Meteorol. 156, 65–74.

Lindroth, A., Mölder, M., Lagergren, F., 2010. Heat storage in forest biomass improves energy balance closure. Biogeosciences 7 (1), 301–313.

Massman, W.J., 2000. A simple method for estimating frequency response corrections for eddy covariance systems. Agric. Forest Meteorol. 104 (3), 185–198.

Mauder, M., Desjardins, R.L., Pattey, E., Gao, Z., van Haarlem, R., 2008. Measurement of the sensible eddy heat flux based on spatial averaging of continuous ground-based observations. Bound. Layer Meteorol. 128 (1), 151–172.

Mauder, M., Foken, T., 2006. Impact of post-field data processing on eddy covariance flux estimates and energy balance closure. Meteorol. Z. 15 (6), 597–609.

Monteith, J.,1965. Evaporation and the environment, the state and movement of water in living organisms. In: Proceedings of the XIX Symposium of Society for Experimental Biology. Cambridge University Press, Swansea, pp. 205–234.

Nadezhdina, N., Ferreira, M., Silva, R., Pacheco, C., 2008. Seasonal variation of water uptake of a *Quercus suber* tree in Central Portugal. Plant Soil 305 (1), 105–119.

Nakai, T., Shimoyama, K., 2012. Ultrasonic anemometer angle of attack errors under turbulent conditions. Agric. Forest Meteorol. 162–163, 14–26.
Papale, D., Reichstein, M., Aubinet, M., Canfora, E., Bernhofer, C., Kutsch, W., Longdoz, B., Rambal, S., Valentini, R., Vesala, T., Yakir, D., 2006. Towards a standardized processing of net ecosystem exchange measured with eddy covariance technique: algorithms and uncertainty estimation. Biogeosciences 3 (4), 571–583.
Richardson, A.D., Hollinger, D.Y., Burba, G.G., Davis, K.J., Flanagan, L.B., Katul, G.G., Munger, J.W., Ricciuto, D.M., Stoy, P.C., Suyker, A.E., Verma, S.B., Wofsy, S.C., 2006. A multi-site analysis of random error in tower-based measurements of carbon and energy fluxes. Agric. Forest Meteorol. 136 (1–2), 1–18.
Sauer, T.J., Horton, R., 2005. Soil heat flux. In: Hatfield, J.L., Baker, J.M., Viney, M.K. (Eds.), Micrometeorology in Agricultural Systems. American Society of Agronomy Inc./Crop Science Society of America Inc./Soil Science Society of America Inc., Madison, WI, USA, pp. 131–154.
Twine, T.E., Kustas, W.P., Norman, J.M., Cook, D.R., Houser, P.R., Meyers, T.P., Prueger, J.H., Starks, P.J., Wesely, M.L., 2000. Correcting eddy-covariance flux underestimates over a grassland. Agric. Forest Meteorol. 103 (3), 279–300.
Widmoser, P., 2009. A discussion on and alternative to the Penman–Monteith equation. Agric. Water Manage. 96 (4), 711–721.
Widmoser, P., 2010. An alternative to define canopy surface temperature bounds. Agric. Water Manage. 97 (2), 224–230.
Williams, C.A., Reichstein, M., Buchmann, N., Baldocchi, D., Beer, C., Schwalm, C., Wohlfahrt, G., Hasler, N., Bernhofer, C., Foken, T., Papale, D., Schymanski, S., Schaefer, K., 2012. Climate and vegetation controls on the surface water balance: synthesis of evapotranspiration measured across a global network of flux towers. Water Resour. Res. 48 (6), W06523.
Williams, M., Richardson, A.D., Reichstein, M., Stoy, P.C., Peylin, P., Verbeeck, H., Carvalhais, N., Jung, M., Hollinger, D.Y., Kattge, J., Leuning, R., Luo, Y., Tomelleri, E., Trudinger, C.M., Wang, Y.P., 2009. Improving land surface models with FLUXNET data. Biogeosciences 6 (7), 1341–1359.
Wilson, K., Goldstein, A., Falge, E., Aubinet, M., Baldocchi, D., Berbigier, P., Bernhofer, C., Ceulemans, R., Dolman, H., Field, C., Grelle, A., Ibrom, A., Law, B.E., Kowalski, A., Meyers, T., Moncrieff, J., Monson, R., Oechel, W., Tenhunen, J., Valentini, R., Verma, S., 2002. Energy balance closure at FLUXNET sites. Agric. Forest Meteorol. 113 (1-4), 223–243.
Wohlfahrt, G., Fenstermaker, L.F., Arnone III, J.A., 2008. Large annual net ecosystem CO_2 uptake of a Mojave Desert ecosystem. Global Change Biol. 14 (7), 1475–1487.
Wohlfahrt, G., Haslwanter, A., Hörtnagl, L., Jasoni, R.L., Fenstermaker, L.F., Arnone III, J.A., Hammerle, A., 2009. On the consequences of the energy imbalance for calculating surface conductance to water vapour. Agric. Forest Meteorol. 149 (9), 1556–1559.
Wohlfahrt, G., Irschick, C., Thalinger, B., Hörtnagl, L., Obojes, N., Hammerle, A., 2010. Insights from independent evapotranspiration estimates for closing the energy balance: a grassland case study. Vadose Zone J. 9 (4), 1025–1033.